PCCP

Surface Chemistry at the Solid-Solid Interface: Mechanically Induced Reaction Pathways of C_8 Carboxylic Acid Monolayers on Copper

Journal:	*Physical Chemistry Chemical Physics*
Manuscript ID	CP-ART-07-2021-003170.R1
Article Type:	Paper
Date Submitted by the Author:	05-Aug-2021
Complete List of Authors:	Rana, Resham; University of Wisconsin-Milwaukee College of Letters and Science, Chemistry and Biochemistry Bavisotto, Robert; University of Wisconsin-Milwaukee College of Letters and Science, Chemistry and Biochemistry Hu, Kaiming ; University of Wisconsin-Milwaukee, Chemistry Tysoe, W.; University of Wisconsin-Madison, Chemistry and Biochemistry

Surface Chemistry at the Solid-Solid Interface: Mechanically Induced Reaction Pathways of C_8 Carboxylic Acid Monolayers on Copper

Resham Rana, Robert Bavisotto, Kaiming Hou and Wilfred T. Tysoe*

Department of Chemistry and Laboratory for Surface Studies, University of Wisconsin-Milwaukee, Milwaukee, WI 53211, USA

Abstract

Mechano- or tribochemical processes are often induced by the large pressures, of the order of 1 GPa, exerted at contacting asperities at the solid-solid interface. These tribochemical process are not very well understood because of the difficulties of probing surface-chemical reaction pathways occurring at buried interfaces. Here, strategies for following surface reaction pathways in detail are illustrated for the tribochemical decomposition of 7-octenoic and octanoic acid adsorbed on copper. The chemistry was measured in ultrahigh vacuum by sliding either a tungsten carbide ball or a silicon atomic force microscope (AFM) tip over the surface to test a previous proposal that the nature of the terminal group in the carboxylic acid, vinyl versus alkyl, could influence its binding to the counterface, and therefore the reaction rate. The carboxylic acids bind strongly to the copper substrate as carboxylates to expose the hydrocarbon terminus. The tribochemical reaction rate was found to be independent of the nature of the hydrocarbon terminus, although the pull-off and friction forces measured by the AFM were different. The tribochemical reaction is initiated in the same way as the thermal reaction, by the carboxylate group tilting to eliminate carbon dioxide and deposit alkyl species onto the surface. This reaction occurs thermally at ~640 K, but tribochemically at room temperature, producing significant differences in the rates and selectivities of the subsequent decomposition pathways of the adsorbed products.

Keywords: carboxylic acids, copper, reaction kinetics, Auger spectroscopy, Atomic force microscopy

* Author to whom correspondence should be addressed.

Introduction

Advances in detailed, mechanistic understanding the chemical processes occurring on surfaces were made using ultrahigh vacuum (UHV) techniques that enabled surfaces to be analyzed by electron-based spectroscopies.[1] This approach was most often used to study catalytic reaction pathways,[2] but suffered from the "pressure gap" because the UHV conditions needed to carry out mechanistic studies were very different from those under which catalytic reactions are carried out. As a result, a number of surface-sensitive techniques were developed that allowed surfaces to be studied in the presence of relatively high gas pressures.[3]

However, perhaps the most difficult surface-chemical challenge is to study reaction pathways at buried, solid-solid interfaces, which are relevant to understanding mechanochemical reactions.[4-8] Thus, while mechanochemical reactions have been known for millennia; for example, the mechanical reduction of cinnabar to mercury in a copper pestle and mortar was reported in ~315 BC, [9] and Faraday studied the mechanochemistry of solids in the 19th century,[10] their reaction pathways are still not well understood. The first theories of mechanical activation of chemical reactions were proposed by Evans and Polanyi [11, 12] who predicted that the reaction rate constant k should vary with hydrostatic pressure P as $k(P) = k_0 \exp\left(\frac{P\Delta V^{\ddagger}}{k_B T}\right)$, where $\Delta V^{\ddagger}$ is known as the activation volume, and is of the order of 10 Å^3/molecule,[13] k_0 is the rate constant at zero (or low) pressure, k_B is the Boltzmann constant and T is the absolute temperature. This became known as the Bell equation,[14] and predicts that pressures of the order of ~1 GPa are required to measurably accelerate the rates of chemical reactions. Such pressures are easily attained at contacting interfaces,[15] implying that mechanochemistry is primarily a field of surface chemistry; mechanochemical reactions are often induced by the large contact stresses occurring in a ball mill [16-22] and the decomposition of molecules added to lubricants are dominated by mechano- or

tribochemical processes,[23-25] although it should be noted that there are other strategies for imposing high enough stresses to influence the rates of chemical reactions.[26]

Methods for elucidating surface reaction pathways at a solid-solid interface are illustrated here using long-chain carboxylic acids (fatty acids), which are used as additives to lubricants and act as so-called friction modifiers by adsorbing on the surface to lower friction,[27-30] but can also decompose during rubbing to form low-friction carbonaceous films.[27, 29, 31-33]

The reaction mechanism of fatty acids with tetrahedral amorphous carbon (ta-C) has been investigated theoretically using a combination of molecular dynamics (MD) simulations with a reactive potential, and first-principles density function theory (DFT) calculations.[28] The simulations reveal that the carboxylic acids bind to one surface via the –COOH functionality, but the presence of an accessible terminal vinyl group on the carbon chain can influence the reactivity by binding to the moving counterface to exert large forces on the bridging molecule, thereby mechanically inducing decomposition. Interestingly, the ability of the vinyl group to interact with the counter-surface, and its mechanochemical reactions, depend on the conformation of the chain. The adsorbed reactant (the fatty acid) can potentially simultaneously bind to the substrate via an attachment point (AP) and to the moving counterface at a pulling point (PP) where the strengths of AP and PP binding relative to the activation energy of tribochemical reaction could control the reactivity.[34] Interactions with the counterface have also recently been suggested to play a role in the mechanochemical etching of silicon.[35] These ideas are scrutinized in the following by selecting molecules that tune the PP functionality while keeping the AP interaction constant using carboxylic acids adsorbed on a copper substrate, which bind strongly to the surface in a bidentate η^2 configuration as a carboxylate [36, 37] at room temperature to provide an AP.

The effect of the PP is measured by comparing the behavior of 7-octenoic (a C_8 hydrocarbon with a terminal C=C group) and octanoic acid (with a C_8 alkyl chain) anchored to a copper foil in ultrahigh vacuum (UHV) to gauge the effect of a vinyl terminal group on reactivity. Tribochemical reaction are induced by rubbing a tungsten carbide ball on the surface, where the use of hard tungsten carbide ensures that the ball will not wear when rubbed against copper, and tungsten and molybdenum carbides have been suggested to have catalytic properties akin to those found for noble metals (platinum and palladium).[38-40] This has been borne out by UHV surface studies that show strong C=C binding by electron donation into the π* antibonding orbitals that also reduces the bond order,[41, 42] implying that the vinyl group will bind strongly to the surface of the tribopin.

Carboxylic acids adsorb on copper by forming η^2-acetate species [36] and decompose by evolving carbon dioxide with the simultaneous formation of hydrocarbon fragments at ~650 K in temperature-programmed desorption (TPD).[43-46] Acetic acid decomposes tribochemically on copper in UHV [47] where the reaction products depend on the direction of the shears stress with respect to the OCO plane of the carboxylate group. Forces that are perpendicular to the plane induce molecular tilting in a direction that is coincident with its journey from the reactant to the transition state for the thermal reaction. Here the acetate species react to evolve gas-phase carbon dioxide and deposit methyl species on the surface. If the shear forces lie within the OCO plane, the stress induces a higher-activation-energy reaction by forming an η^1-acetate intermediate that produces carbon monoxide and adsorbed oxygen instead.

Previous work has studied the thermal surface chemistry of octanoic [48] and 7-octenoic acid [49] on a copper foil and a Cu(100) single crystal using a combination of reflection-absorption infrared spectroscopy (RAIRS), TPD, X-ray photoelectron spectroscopy (XPS) and scanning-tunneling microscopy (STM). Both carboxylic acids adsorb as bidentate carboxylates at room temperature.

The carbon chain of 7-octenoate is oriented away from the surface, but starts to tilt on heating, to induce C–COO scission to produce a small amount of carbon dioxide at ~600 K. Most of the decarboxylation occurs at ~650 K when CO_2 and hydrogen evolve simultaneously. Approximately half of the carbon is deposited on the surface as oligomeric species that undergo further dehydrogenation to evolve more hydrogen at ~740 K. This leaves a carbonaceous layer on the surface, which contains hexagonal motifs connoting the onset of graphitization of the surface.[49]

Similar chemistry occurs for octanoate species, which bind with the alkyl group parallel to the surface with a tilted carboxylate group at low coverages.[48] The flat-lying structure facilitates octanoate decomposition by desorbing carbon dioxide at ~550 K. Increasing the octanoate coverage causes the alkyl chains to be more perpendicular to the surface, which stabilizes the adsorbate. It decomposes by desorbing carbon dioxide at ~640 K, where infrared spectroscopy confirms that this also occurs by the carboxylate tilting towards the surface. The resulting heptyl species can either decompose by desorbing hydrogen or can also polymerize on the surface.

The tribo- mechanochemistry is investigated here in ultrahigh vacuum either using a ball-on-flat geometry by monitoring the elemental composition in the rubbed regions by Auger spectroscopy, or by using an atomic force microscopy (AFM) tip by measuring the depth of the groove formed by rubbing.

Experimental Methods

Experiments were carried out in stainless-steel, ultrahigh vacuum (UHV) chambers operating at base pressures of ~2×10^{-10} Torr following bakeout for the surface analyses of the carboxylic acids,[50] for tribological measurement,[51] and for AFM experiments.[52] Briefly, the tribology chamber was equipped with a UHV-compatible tribometer, which simultaneously measures

normal load, lateral force and the electrical contact resistance between the tip and substrate. All tribological measurements were made using a sliding speed of ~4×10^{-3} m/s at a normal load of 0.44 N. Previous work has shown that the maximum interfacial temperature rise for a copper sample under these conditions is much less than 1 K.[53] The spherical tribopin (~1.27×10^{-2} m diameter) was made from tungsten carbide containing some cobalt binder and could be heated by electron bombardment in vacuo, or by argon ion bombardment, in order to clean it. The pin was attached to an arm that contained strain gauges to enable the normal and lateral forces to be measured. The arm was mounted to a rotatable $2\frac{3}{4}$" Conflat flange to allow the pin to face a cylindrical mirror analyzer (CMA) to enable Auger spectra of the pin surface to be collected. Additional experiments were carried out by analyzing the tungsten carbide pin by XPS after argon ion bombardment using a spectrometer containing a hemispherical analyzer built by ThermoFisher (220i) with a focused monochromatic X-Ray source.[54]

The copper foil samples (Alfa Aesar, 99.99% pure, 1 mm thick) were polished to a mirror finish using 1 μm diamond paste and then rinsed with deionized water and degreased ultrasonically in acetone before mounting in the UHV chamber. The copper was cleaned using a standard procedure which consisted of argon ion bombardment (~1 kV, ~2 μA/cm^2) and annealing cycles and the cleanliness of the samples was monitored using Auger spectroscopy.

The tribometer chamber contained a single-pass CMA for Auger analysis, and an argon ion bombardment source for sample cleaning and depth profiling. Auger spectra were either collected using the coaxial electron gun in the CMA with an electron beam energy of 3 kV or with a Staib model EK050M2 Microfocus electron gun. The chamber was also equipped with a channeltron secondary-electron detector, which allowed scanning electron microscopy (SEM) images of the

rubbed region to be collected using the high-resolution electron gun, which also enabled Auger elemental profiles to be obtained across the wear track.

Experiments were performed by initially rubbing the tribopin against the clean copper foil (~1.7 × 1.7 cm^2 by ~ 1 mm thick) until a constant friction coefficient was obtained. This resulted in the formation of a wear track. The carboxylic acids were dosed through a Knudsen source connected to a dosing tube (with an internal diameter of 4×10^{-3} m) directed towards the sample so that the pressure at the sample is enhanced compared to the measured background pressure, where pressures are not corrected for ionization gauge sensitivity.

AFM experiments were carried out using an RHK Variable Temperature UHV 750 atomic force microscope (AFM) operating at a base pressure of ~2×10^{-10} Torr following bakeout. The apparatus also contained an analysis chamber for sample cleaning and was equipped with a Scienta Omicron SPECTALEED combined low-energy electron diffraction (LEED)/Auger system for assessing sample cleanliness and crystalline order. The chamber was also equipped with a Dycor quadrupole mass analyzer for leak checking and background gas analysis. The Cu(100) single crystal was cleaned by argon ion bombardment (~1 kV, ~2 μA/cm^2) and then by annealing to ~850 K to remove any surface damage induced by the cleaning procedure. A saturated overlayer of carboxylic acids was prepared in the same way as for the experiments in the UHV tribometer.

Stress-induced mechanochemical reaction kinetics were measured by applying a normal force using a silicon μ-masch (HQ:NSC19/NO AL) AFM tip with a nominal 8 nm radius. The cantilever force constant was obtained both from the geometry of the cantilever measured by scanning electron microscopy [55] and by using a implementation of a method first proposed by Sader.[56] Both methods yielded identical results. Attempts were made to perform these experiments using tungsten carbide AFM tips, but they turned out to be too brittle for repeated use. However, both

the pull-off and friction forces measured by a silicon tip depended on the nature of the carboxylate overlayer so that these experiments still allowed reaction rates and tip-surface interactions to be compared.

Because the pressure varies as a function of distance from the centre of the contact for elastic contact of a spherical tip on a planar substrate,[57] the pressure at the centre of the contact was estimated from indentation measurements on thiolate-covered copper.[52] Force-distance curves were measured between each rubbing experiment to verify that the tip shape had not changed.

The 7-octenoic acid (Sigma Aldrich, ≥96.5% purity), octanoic acid (Sigma Aldrich, ≥98.0% purity), 6-heptenoic acid (Sigma Aldrich, ≥98.5% purity) and heptanoic acid (Sigma Aldrich, ≥99.0% purity) were transferred to glass bottles and attached to the gas-handling system of the vacuum chamber, where they were subjected to several freeze-pump-thaw cycles.

Results

Tribochemical experiments were carried out by rubbing a carboxylate-covered surface with a cleaned tungsten carbide ball in UHV. Auger and XPS analyses of the pin surface (Figure 1) confirm that the surface of the pin comprises tungsten carbide after heating or argon-ion bombardment in UHV and will be able to bind to the vinyl group terminus of 7-octenoic acid.

The rubbed region was analyzed using small-spot-size Auger spectroscopy. Attempts were made to monitor the gas-phase products formed during sliding as done previously,[58-60] but the residual background mass-spectrometer signal after sample dosing precluded such experiments from being carried out. Figure 2 shows the results of experiments carried out on a saturated overlayer of 7-octenoic acid on copper. Here the clean surface was first rubbed to create a wear track and then saturated with 7-octenoic acid, where the saturation dose was gauged by measuring

the C KLL Auger spectral intensity as a function of exposure. This yields a C/Cu peak-to-peak ratio of ~0.65 obtained using the microfocus electron gun. The decrease in the amount of carbon on the surface as it is rubbed (■) indicates that the adsorbed 7-octenoate reacts tribochemically. The signal decreases to a final C/Cu Auger ratio of ~0.12 after ~35 passes and a fit to an exponential decrease yields a number of passes to reduce the signal by 1/e, $S_e = 7.9 \pm 1.1$ scans. The exponential decay in carbon Auger signal implies a first-order decomposition rate.

The experiment was repeated without cleaning the substrate or the pin (Fig. 2, ●) to assess how the presence of carbonaceous products influenced the reaction kinetics. The results show that the signal decay rate is approximately identical to the first experiment, but that there is a slight increase in the amount of carbon on the surface (to a C/Cu ratio of 0.14 after the second scan). In order to investigate this further, the surface was repeatedly dosed and rubbed until the carbon Auger signal intensity remained constant. The results are displayed in Figure 3 for 7-octenoic acid adsorption. Here, the amount of carbon on the surface increases significantly after the surface had been dosed and rubbed 4 times to yield a C/Cu ratio of 0.26 at a rate of 0.047 ± 0.008 C/Cu per scan, and then does not change. The amount of carbon initially on the surface after dosing the sample with 7-octenoic acid decreases as the surface becomes covered by carbon (note that this is the sum of the carbon deposited during the previous cycles plus the 7-octenoic acid then adsorbed). The results also imply that the tribochemical reaction for a surface that accumulates sufficient carbon to yield a C/Cu ratio of 0.26 results in the deposition of no more additional carbon. This indicates that 7-octenoate decomposes on, or desorbs from this surface to yield only gas-phase products. Since a saturated overlayer of 7-octenoic acid has a C/Cu Auger ratio of 0.65, the additional carbon formed after ≥5 dose-and-rub cycles (the difference between the signal for the saturated overlayer with a

C/Cu Auger ratio of 0.59 and the surface after rubbing with a C/Cu Auger ratio of 0.26) corresponds to a relative coverage of ~0.56 monolayer of 7-octenoate species.

A similar sequence of experiments was carried out on a copper surface dosed with octanoic acid. Because of the absence of any unsaturated groups in the chain that could bind strongly to the tungsten carbide pin, it is anticipated that it will be less tribochemically reactive than a 7-octenoate overlayer, which has a terminal vinyl group. The variation in C/Cu Auger ratio as a function of the number of rubbing cycles is shown in Figure 4. Approximately the same amount of carbon is deposited onto the surface at the end of 50 rubbing cycles, with a C/Cu Auger ratio of ~0.11, but S_e decreases to 1.8 ± 0.2 scans, a much faster rate than for 7-octenoic acid (Fig. 2), apparently contradicting the prediction from MD simulations.[28] The effect of repeated dosing is shown in Fig. 5, where there is a significant blocking of the surface by the reaction products, and the final amount of carbon (corresponding to a C/Cu Auger ratio of 0.27) is the same as for 7-octenoic acid. The amount of carbon on a surface dosed with octanoic acid increases at a rate of 0.042 ± 0.004 C/Cu per dose, similar to that found for 7-octenoic acid (Fig. 3).

The rates of the removal are summarized in Table 1 for the carboxylic acids studied here compared with acetic acid.[47] It is evident that the carbon signal decreases much more rapidly as a function of the number of times that the sample had been rubbed for an alkyl-terminated carboxylic acid (octanoic acid) than one having a terminal vinyl group (7-octenoic acids).

Surface chemistry experiments indicate that the thermal reaction involves the formation of carbon dioxide from the carboxylate group, followed by a reaction of the resulting hydrocarbon fragment so that carbon removal occurs in several steps.[48, 49] To disentangle these effects, the loss of oxygen from the surface as a function of the number of passes was also monitored and the results are displayed in Figure 6, which also includes additional results for 6-heptenoic acid (▲) and

heptanoic acid (▼) on copper. Note that the oxygen Auger signal is much smaller than the carbon signal because there is much more carbon than oxygen in the adsorbed layer and the oxygen is located at the surface, while the carbon is in the outermost layer. The amount of oxygen decreases at an identical rate for all carboxylate overlayers, at $S_e =$ 2.0 ± 0.1 scans, similar to the rate of carbon removal from octanoic acid (Table 1). This implies that there is little effect of varying the nature of the outermost functionality, and thus the nature of the pulling point, on the overall shear-induced rate of decomposition of the carboxylic acids. This indicates that any difference in the rates of carbon removal must be due to differences in the rates at which the resulting hydrocarbon fragments react.

Frictional Behavior of Carboxylic Acids on Copper

The evolution of the friction coefficient as a function of the number of passes for a 7-octenoic acid overlayer on clean copper is shown in Figure 7. The presence of the 7-octenoic acid on the surface significantly reduces the initial friction coefficient to 0.32 ± 0.02 (■, Table 1), due to the presence of the carbonaceous species on the surface discussed above, which remains constant at this value for ~8 scans, and then starts to increase to reach a final asymptotic value of 0.49 ± 0.02, close to the friction coefficient for clean copper after a run-in period,[53, 58, 61] where the friction coefficient rises logarithmically to the clean-surface value with a characteristic number of scans of 13 ± 1. The corresponding variation in friction coefficient after the surface had been dosed six times with 7-octenoic and rubbed for 50 scans is also shown (●). Here the initial friction coefficient is reduced to 0.20 ± 0.02 due to the presence of additional carbonaceous species on the surface and (Fig. 3) and then rises exponentially at approximately the same rate as for the first dose.

Similar behavior is seen for an octanoic acid overlayer on copper (Figure 8) where the initial friction coefficient is 0.24 ± 0.02 (■), and remains constant at this value for ~4 scans. Note that the number of scans for the initial constant friction correlates with the carbon removal rates (Figs. 2 and 4), suggesting that the carboxylate overlayers have approximately the same values of friction while they are being removed, and the friction of the film only starts to increase as subsequent sliding causes dehydrogenation and reorganization of the adsorbed carbonaceous species.[48, 49] The friction coefficient then rises to 0.52 ± 0.01, again consistent with the friction coefficient of a clean surface. The overlayer on a substrate that has been dosed with octanoic acid and rubbed six times again has a significantly lower initial friction coefficient of 0.15 ± 0.01, and has a broadly similar behavior to 7-octenoic acid, and again rises to the clean-surface value after ~50 scans.

Reactions Induced by an AFM Tip

In order to directly compare the tribochemical reaction rates with the strengths of interaction between the tip and the carboxylate overlayers, experiments were carried out using an AFM tip with a nominal radius of ~8 nm at an applied normal load of nN. Based on previous calibrations,[52] this corresponds to a normal stress at the center of the contact of ~0.27 GPa.

Cu(100) samples, covered by saturated overlayers of either octanoic or 7-octenoic acid, were rubbed with an AFM tip at ~120 nm/s, and the depth of the worn region imaged periodically using a non-perturbative load to measure the depth at the center of the worn region. The results are displayed in Fig. 9, which show that a groove is formed, which increases in depth with the number of scans. The resulting traces can be fit to an exponential, suggesting first-order kinetics, agreeing with the tribometer experiments (Figs. 2 and 4). The characteristic time for the removal of the octanoate overlayer (■) is 610 ± 16 scans and is close to that found for the removal of 7-octenoates

(●) of 590 ± 20 scans. These results are in accord with the data in Fig. 6 showing that the rates of oxygen removal were identical for all carboxylates, independent of the nature of the terminus and proposed interactions with the counterface.

The asymptotic depths are 360 ± 5 pm for the octanoate layer and 300 ± 10 pm for the 7-octenoate film. These values are significantly less that the thickness of these adsorbed C_8 films of ~1000 pm estimated from density functional theory calculations.[48, 49] The difference likely arises from two sources. First is the compliance of the soft film which could lead to an underestimate of the groove depth. Second, as indicated by the Auger analyses, carbon remains on the surface after it has been rubbed so that the bottom of the groove is not the Cu(100) substrate.

To investigate whether the similarity in film removal rates is a result of both carboxylate films interacting similarly with the tip, the pull-off forces are compared in Fig. 10, plotted as a distribution of repeated measurements. They yield quite different values of the pull-off forces of 14 ± 4 nN for an octanoate overlayer compared with 31 ± 5 nN for the 7-octenoate, consistent with the terminal C=C group in the 7-octenoate overlayer interacting more strongly than the saturated alkyl terminus of the octanoate film. This, however, does not seem to influence the reaction rates.

The friction forces were also compared and the results are displayed as a function of the number of scans in Fig. 11. This shows larger friction forces for a 7-octenoate overlayer (of 19.30 ± 0.04 arbitrary units (a.u)) than for an octanoate film with a friction force of 7.95 ± 0.02 a.u. Interestingly, the ratio of pull-off forces for 7-octenoic and octanoic acids of ~2.33 is very close to the ratios of their friction forces of 2.43 measured by AFM. The friction forces measured by AFM (Fig. 11) do not change as the adsorbates react (Fig. 9), which is similar to the behavior found in the UHV tribometer (Figs. 7 and 8), confirming that the overlayers have constant friction until they have all been removed and implies that the stresses at the AFM tip are not sufficiently large to induce the

larger increases in friction as found at higher numbers of rubbing cycles observed in the UHV tribometer (see Figs. 7 and 8).

Discussion

The results indicate that medium-chain-length carboxylic acids adsorbed on copper undergo tribochemical reactions to deposit carbonaceous species on the surface. In addition to carboxylic acids functioning as friction modifiers by forming protective adsorbed molecular overlayers,[30] they can react at the interface to form lubricious carbonaceous films [27, 31, 32] and thus also function as friction-reducing additives. An important conclusion from this work is that the reaction is mechanochemically induced rather than being accelerated by some other process such as interfacial heating since the temperature rise during sliding on copper under the conditions used here is negligible.[62] This is in accord with the predictions from simulations [28] and it is a common feature of lubricant additives that their reactions are mechanochemically driven as, for example, for zinc dialkyl dithiophosphate (ZDDP) and phosphate esters.[23, 24, 63]

The tribochemical reaction is initiated by the cleavage of the bond between the carboxylate anchoring group and the hydrocarbon chain to form carbon dioxide that rapidly desorbs from the surface [47] as indicated by the loss of oxygen (Fig. 6). This results in the formation of a hydrocarbon radical, which then subsequently reacts to deposit carbonaceous species on the surface, that reduces friction.[64] The oxygen removal rates for octanoic and 7-heptenoic acids of 2.1 ± 0.1 per pass are significantly faster than those found for acetate species on copper [47] of 6.6 ± 0.5 per pass, and suggest that the presence of longer carbon chains facilitates tribochemical C–C bond scission. Surface chemical studies of both octanoic [48] and 7-octenoic [49] acids on copper indicate that the termini of the hydrocarbon groups of these carboxylic acids are sufficiently long and flexible to

access the copper substrate thereby causing the carboxylate group to tilt to approach the configuration in the activated complex.[47] This facilitates carboxylate decomposition and is expected to occur more easily for long-chain hydrocarbons than for short-chain ones. Note that oxygen has been completely removed after eight scans for long-chain hydrocarbons (Fig. 6), while some oxygen remained after rubbing an acetate-covered surface [47] due to a higher-energy pathway being tribochemically induced that involves the shear-induced formation of an η^1-intermediate. This implies that chain-surface interactions facilitate molecular tilting in a direction that increases the tribochemical reaction selectivity to favor the lowest-energy pathway.

As discussed above, it has been postulated that the interaction between the terminus of the hydrocarbon chain and the moving counterface (the pulling point) might influence the tribochemical reaction rate, where the stronger binding of a vinyl than an alkyl group to the tungsten carbide surface should result in higher forces being exerted, resulting in higher reactivity.[28] The experimental results presented here suggest that the tribochemical decomposition rates of adsorbed carboxylates are independent of the nature of the terminal group for the ball-on-flat contact used in this work.

This was further investigated by using a nominal ~8 nm-radius AFM silicon tip at a normal applied load of 56 nN to produce a contact stress of ~0.27 GPa. This is in the same range of the contact pressures in the ball-on-flat geometry in the UHV tribometer estimated to be between 0.1 and 0.4 GPa depending on the choice of contact model.[62] The rates of reaction are the also same for both octanoic and 7-octenoic acid at the nanoscale (Fig. 9), in accord with the results obtained with similar values of normal stress in UHV tribometer. This equipment allows the tip-surface interactions to be measured directly from the pull-off forces (Fig. 10) to indicate that the tip-surface interaction is stronger for a 7-octenoate-covered surface than an octanoate-covered one due to the

presence of the vinyl terminal group in the 7-octenoate overlayer on copper. This also influences the friction forces for the saturated and unsaturated overlayers (Fig. 11), where the unsaturated carboxylate overlayer has higher friction than the saturated carboxylate, and the values scale with the corresponding pull-off forces. Similarly higher friction forces were observed previously for unsaturated acids (containing C=C groups) than for saturated carboxylic acid,[65, 66] but were explained by the fact that the unsaturated carboxylic acid is more loosely packed on the surface.

The nanoscale friction coefficient remains constant during carboxylate decomposition (Fig. 11) indicating that the low-temperature decomposition of the overlayers does not influence the frictional properties, a useful characteristic for a friction-modifying overlayer. This behavior is also observed in the UHV tribometer friction measurements (Figs. 7 and 8), where the friction coefficient remains constant while the adsorbed carboxylates are undergoing shear-induced decomposition, but then increases as rubbing continues. A possible explanation is that the resulting hydrocarbonaceous species resemble the parent hydrocarbon chain in the overlayer, leading to similar friction until it undergoes further tribochemical reactions to remove hydrogen and form strongly bound carbonaceous deposits on the surface. They are also eventually removed to cause the friction to rise to the clean-surface value after long rubbing times in the UHV tribometer. However, this appears to produce some residual effect since the initial friction is lower after six dose-and-rub cycles than after the first cycle.

Despite the similar rates of tribochemical decomposition of carboxylate species on copper, there are significant differences in the relative rates of carbon loss (compare Figs. 2 and 4). In the case of octanoic acid, the initial rate of carbon removal ($S_e = 1.8 \pm 0.2$ scans, Fig. 4 and Table 1) is essentially identical to the rate of oxygen removal (Fig. 6), indicating that a portion of the resulting alkyl species react very rapidly once it has been formed. The surface chemistry of alkyl

species has been studied on copper and they react either by β-hydride elimination to form an alkene, or hydrogenate to an alkane. Both reactions occur below room temperature.[67, 68] The resulting alkyl species can also oligomerize and this process has been imaged on surfaces that have been heated to high temperatures to thermally decompose the carboxylate species.[48, 49, 64] However, the data shown in Table 2 emphasize that the amount of carbon formed by thermal or tribological treatments are significantly different, where ~36% of the carbon remains on the surface after heating an octanoate-covered copper surface, while only ~11% remains after rubbing. The coverage of thermally deposited carbon for long-chain hydrocarbons is also significantly larger than for the thermal decomposition of acetate species.[45, 69] This difference can be rationalized by nothing that hydrocarbon fragments are generated thermally on copper at temperatures between 630 and 640 K, while they are tribochemically formed at 300 K. This will influence the reaction selectivity such that lower-activation-energy reactions are tribologically favored relative to higher-activation-energy ones. Since the most facile reaction is β-hydride elimination of heptyl groups to desorb 1-heptene, which effectively removes carbon from the surface, inducing other (dehydrogenation of oligomerization) pathways at higher temperatures will result in more carbon being deposited on the surface.

The 7-octenoate reaction is slower ($S_e =$ 7.9 ± 1.1 scans, Fig. 4 and Table 1) than the tribochemical decomposition of either acetic acid or octanoic acid, while the rate of oxygen removal is rapid (Fig. 6). This indicates that a hydrocarbon fragments with the terminal C=C groups react more slowly than those with an alkyl terminus. This is proposed to be because the terminal vinyl group can also interact with the surface to stabilize the hydrocarbon fragment.[64] This result confirms that the thermal and tribological reactivities of carboxylic acids, at least on

copper, depend on the temperature at which the hydrocarbon fragments are formed; at a high temperature for the thermal reaction, but close to room temperature for the tribochemical process.

The evolution of the surface as a function of the number of times that it is dosed and rubbed is compared in Figures 3 and 5. Note that the points denoted ’50 scans’ in both plots show the C/Cu Auger ratios after the saturated surfaces had been rubbed 50 times, when the composition of the surface no longer changes, and the points denoted ‘0 scans’ indicate the C/Cu Auger signal after the surface has been saturated with the carboxylic acid at 300 K. Thus, the amount of carbon on the surface after rubbing evolves in a similar manner for both carboxylic acids when the C/Cu Auger ratio changes by ~0.042 per pass to saturate at a value of ~0.27, corresponding to a relative coverage of ~0.4 of the saturation coverage on the clean surface. These ratios remain constant after four dose-and-rub cycles indicating that all additional carboxylate species present on this carbonaceous layer on copper are completely removed. This surface therefore appears to be self-healing so that, when carbon is removed from the surface, it will be reactively replenished. Curiously, the resulting carbonaceous layer seems to be more effective at blocking the subsequent adsorption of octanoic acid (Fig. 5, where it accommodates ~0.5 ML) than 7-octenoic acid (Fig.3, where it adsorbs ~0.25 ML).

Conclusions

The surface tribo/mechanochemistry of anchored carboxylic acids is studied in UHV at a solid-solid contact using either a tungsten carbide ball or a silicon AFM tip sliding against an adsorbate-covered copper surface to illustrate the strategies that can be used to follow reaction mechanisms at inaccessible solid-solid interfaces. These approaches are used to investigate the influence of the terminus of anchored C_8 carboxylates on a copper substrate to compare with theoretical predictions

based on quantum calculations and first principles MD simulations that suggest that different functionalities at the pulling point of the molecule, here the terminus of the hydrocarbon chain, should have a strong influence on the tribochemical reaction rate. Tungsten carbide was selected as the counterface material in the UHV tribometer, and a silicon tip was used in the AFM, and both showed that the carboxylic acid decomposed with identical rates, despite the pull-off and friction forces measured in the AFM being different.

The different tribo-induced carbon removal rates of the two molecules was found to be due to the differences in reactivity of the carbonaceous species deposited onto the surface by carbon dioxide elimination. This causes a different reactivity compared to the thermal reactions because the hydrocarbon fragments are tribologically formed at room temperature, but formed thermally at ~650 K. Thus, the influence of the presence of a terminal vinyl group lies not in its effect on the initial reactivity, but its influence on the reactivity of the tribologically formed species, where the terminal vinyl group is proposed to ligate to the surface, thereby facilitating subsequent dehydrogenation steps, while adsorbed alkyl species can undergo a facile β-hydride elimination reaction to yield the corresponding 1-alkene.

Such strategies will enable the elementary chemical reaction steps occurring in tribo- and mechanochemical reactions to be elucidated, and will form the basis for developing precise models for describing their reactivity, thus offering the possibility of placing the fields of tribochemistry and mechanochemistry on a firm theoretical footing.

Acknowledgements

We gratefully acknowledge the Civil, Mechanical and Manufacturing Innovation (CMMI) Division of the National Science Foundation under grant numbers CMMI-2020525 for support of this work. KH acknowledges support from the China Scholarship Council.

References

1. G. A. Somorjai, *Chemistry in two dimensions surfaces*, Cornell Univ. Pr., Ithaca, 1981.
2. G. Ertl, *Angewandte Chemie International Edition*, 2008, **47**, 3524-3535.
3. D. P. Woodruff, *Surface Science*, 2016, **652**, 4-6.
4. G. A. Bowmaker, *Chemical Communications*, 2013, **49**, 334-348.
5. Z. Huang and R. Boulatov, *Chemical Society Reviews*, 2011, **40**, 2359-2384.
6. R. Boulatov, *Nature Chemistry*, 2013, **5**, 84-86.
7. S. L. James, C. J. Adams, C. Bolm, D. Braga, P. Collier, T. Friscic, F. Grepioni, K. D. M. Harris, G. Hyett, W. Jones, A. Krebs, J. Mack, L. Maini, A. G. Orpen, I. P. Parkin, W. C. Shearouse, J. W. Steed and D. C. Waddell, *Chemical Society Reviews*, 2012, **41**, 413-447.
8. M. D. Eddleston, M. Arhangelskis, T. Friscic and W. Jones, *Chemical Communications*, 2012, **48**, 11340-11342.
9. H. J. Theophrastus, *Theophrastus's history of stones : with an English version, and critical and philosophical notes, including the modern history of the gems, &c., described by that author, and of many other of the native fossils*, London, 1774.
10. M. M. J. K. Faraday, *Chemical manipulation : being instructions to students in chemistry on the methods of performing experiments of demonstration or of research with accuracy and success*, Carey and Lea, Philadelphia, 1831.

11. M. G. Evans and M. Polanyi, *Transactions of the Faraday Society*, 1938, **34**, 11-24.

12. M. G. Evans and M. Polanyi, *Transactions of the Faraday Society*, 1935, **31**, 875-894.

13. A. Drljaca, C. D. Hubbard, R. van Eldik, T. Asano, M. V. Basilevsky and W. J. le Noble, *Chemical Reviews*, 1998, **98**, 2167-2290.

14. G. Bell, *Science*, 1978, **200**, 618-627.

15. M. H. Müser, W. B. Dapp, R. Bugnicourt, P. Sainsot, N. Lesaffre, T. A. Lubrecht, B. N. J. Persson, K. Harris, A. Bennett, K. Schulze, S. Rohde, P. Ifju, W. G. Sawyer, T. Angelini, H. Ashtari Esfahani, M. Kadkhodaei, S. Akbarzadeh, J.-J. Wu, G. Vorlaufer, A. Vernes, S. Solhjoo, A. I. Vakis, R. L. Jackson, Y. Xu, J. Streator, A. Rostami, D. Dini, S. Medina, G. Carbone, F. Bottiglione, L. Afferrante, J. Monti, L. Pastewka, M. O. Robbins and J. A. Greenwood, *Tribology Letters*, 2017, **65**, 118.

16. P. Bellon and R. S. Averback, *Physical Review Letters*, 1995, **74**, 1819-1822.

17. C. Suryanarayana, *Progress in Materials Science*, 2001, **46**, 1-184.

18. B. Rodríguez, A. Bruckmann, T. Rantanen and C. Bolm, *Advanced Synthesis & Catalysis*, 2007, **349**, 2213-2233.

19. G. Kaupp, *Journal of Physical Organic Chemistry*, 2008, **21**, 630-643.

20. V. Sepelak, S. Begin-Colin and G. Le Caer, *Dalton Transactions*, 2012, **41**, 11927-11948.

21. D. Tan and F. García, *Chemical Society Reviews*, 2019, **48**, 2274-2292.

22. C. C. Piras, S. Fernández-Prieto and W. M. De Borggraeve, *Nanoscale Advances*, 2019, **1**, 937-947.

23. N. N. Gosvami, J. A. Bares, F. Mangolini, A. R. Konicek, D. G. Yablon and R. W. Carpick, *Science*, 2015, **348**, 102-106.

24. J. Zhang and H. Spikes, *Tribology Letters*, 2016, **63**, 1-15.

25. J. Zhang, J. P. Ewen, M. Ueda, J. S. S. Wong and H. A. Spikes, *ACS Applied Materials & Interfaces*, 2020, **12**, 6662-6676.

26. G. Cravotto, E. C. Gaudino and P. Cintas, *Chemical Society Reviews*, 2013, **42**, 7521-7534.

27. M. I. De Barros Bouchet, J. M. Martin, C. Forest, T. le Mogne, M. Mazarin, J. Avila, M. C. Asensio and G. L. Fisher, *RSC Advances*, 2017, **7**, 33120-33131.

28. T. Kuwahara, P. A. Romero, S. Makowski, V. Weihnacht, G. Moras and M. Moseler, *Nature Communications*, 2019, **10**, 151.

29. S. Campen, J. H. Green, G. D. Lamb and H. A. Spikes, *Tribology Letters*, 2015, **57**, 18.

30. H. Spikes, *Tribology Letters*, 2015, **60**, 5.

31. M. I. De Barros Bouchet, J. M. Martin, J. Avila, M. Kano, K. Yoshida, T. Tsuruda, S. Bai, Y. Higuchi, N. Ozawa, M. Kubo and M. C. Asensio, *Scientific Reports*, 2017, **7**, 46394.

32. M. Kano, J. M. Martin, K. Yoshida and M. I. De Barros Bouchet, *Friction*, 2014, **2**, 156-163.

33. S. M. Lundgren, M. Ruths, K. Danerlöv and K. Persson, *Journal of Colloid and Interface Science*, 2008, **326**, 530-536.

34. A. M. Khan, H. Wu, Q. Ma, Y.-W. Chung and Q. J. Wang, *Tribology Letters*, 2019, **68**, 6.

35. L. Chen, J. Wen, P. Zhang, B. Yu, C. Chen, T. Ma, X. Lu, S. H. Kim and L. Qian, *Nature Communications*, 2018, **9**, 1542.

36. B. A. Sexton, *Chemical Physics Letters*, 1979, **65**, 469-471.

37. J. James, D. K. Saldin, T. Zheng, W. T. Tysoe and D. S. Sholl, *Catalysis Today*, 2005, **105**, 74-77.

38. R. B. Levy and M. Boudart, *Science*, 1973, **181**, 547-549.

39. L. H. Bennett, J. R. Cuthill, A. J. McAlister, N. E. Erickson and R. E. Watson, *Science*, 1974, **184**, 563-565.

40. S. T. Oyama, *Catalysis Today*, 1992, **15**, 179-200.

41. H. H. Hwu and J. G. Chen, *Chemical Reviews*, 2005, **105**, 185-212.

42. J. B. Benziger, E. I. Ko and R. J. Madix, *Journal of Catalysis*, 1978, **54**, 414-425.

43. H.-P. Lin, Z.-X. Yang, S.-H. Lee, T.-Y. Chen, Y.-J. Chen, Y.-H. Chen, G.-J. Chen, S.-X. Zhan and J.-L. Lin, *The Journal of Chemical Physics*, 2019, **150**, 164703.

44. O. Karis, J. Hasselström, N. Wassdahl, M. Weinelt, A. Nilsson, M. Nyberg, L. G. M. Pettersson, J. Stöhr and M. G. Samant, *The Journal of Chemical Physics*, 2000, **112**, 8146-8155.

45. M. Bowker and R. J. Madix, *Applications of Surface Science*, 1981, **8**, 299-317.

46. N. Canning and R. J. Madix, *The Journal of Physical Chemistry*, 1984, **88**, 2437-2446.

47. R. Rana, R. Bavisotto, N. Hopper and W. T. Tysoe, *Tribology Letters*, 2021, **69**, 32.

48. R. Bavisotto, R. Rana, N. Hopper and W. T. Tysoe, *Surface Science*, 2021, **711**, 121875.

49. R. Bavisotto, R. Rana, N. Hopper, D. Olson and W. T. Tysoe, *Physical Chemistry Chemical Physics*, 2021, **23**, 5834-5844.

50. M. Kaltchev, A. W. Thompson and W. T. Tysoe, *Surface Science*, 1997, **391**, 145-149.

51. F. Gao, O. Furlong, P. V. Kotvis and W. T. Tysoe, *Tribology Letters*, 2008, **31**, 99-106.

52. A. Boscoboinik, D. Olson, H. Adams, N. Hopper and W. T. Tysoe, *Chemical Communications*, 2020, **56**, 7730-7733.

53. O. Furlong, B. Miller and W. Tysoe, *Tribology Letters*, 2011, **41**, 257-261.

54. R. Rana, D. Long, P. Kotula, Y. Xu, D. Olson, J. Galipaud, T. LeMogne and W. T. Tysoe, *ACS Applied Materials & Interfaces*, 2021, **13**, 6785-6794.

55. E. Meyer, H. J. Hug and R. Bennewitz, *Scanning probe microscopy : the lab on a tip*, Springer, Berlin; London, 2011.

56. S. M. Cook, K. M. Lang, K. M. Chynoweth, M. Wigton, R. W. Simmonds and T. E. Schäffer, *Nanotechnology*, 2006, **17**, 2135-2145.

57. K. L. Johnson, Cambridge University Press, Cambridge; New York, 1985.

58. O. J. Furlong, B. P. Miller, P. Kotvis and W. T. Tysoe, *ACS Applied Materials & Interfaces*, 2011, **3**, 795-800.

59. B. Miller, O. Furlong and W. Tysoe, *Tribology Letters*, 2013, **49**, 39-46.

60. H. Adams, B. P. Miller, P. V. Kotvis, O. J. Furlong, A. Martini and W. T. Tysoe, *Tribology Letters*, 2016, **62**, 1-9.

61. O. Furlong, B. Miller and W. T. Tysoe, *Wear*, 2012, **274–275**, 183-187.

62. H. L. Adams, M. T. Garvey, U. S. Ramasamy, Z. Ye, A. Martini and W. T. Tysoe, *The Journal of Physical Chemistry C*, 2015, **119**, 7115-7123.

63. F. Gao, O. Furlong, P. V. Kotvis and W. T. Tysoe, *Langmuir*, 2004, **20**, 7557-7568.

64. R. Bavisotto, R. Rana, N. Hopper, K. Hou and W. T. Tysoe, *PCCP*, 2021, In press

65. M. Doig, C. P. Warrens and P. J. Camp, *Langmuir*, 2014, **30**, 186-195.

66. M. H. Wood, M. T. Casford, R. Steitz, A. Zarbakhsh, R. J. L. Welbourn and S. M. Clarke, *Langmuir*, 2016, **32**, 534-540.

67. C. J. Jenks, C. M. Chiang and B. E. Bent, *Journal of the American Chemical Society*, 1991, **113**, 6308-6309.

68. C. J. Jenks, B. E. Bent and F. Zaera, *The Journal of Physical Chemistry B*, 2000, **104**, 3017-3027.

69. M. Bowker and R. J. Madix, *Surface Science*, 1982, **116**, 549-572.

Tables

Compound	Carbon Removal Rate/S_e Scan	Friction Coefficient
7-Octenoic Acid	7.9 ± 1.1	0.32 ± 0.02
Octanoic Acid	1.8 ± 0.2	0.24 ± 0.02
Acetic Acid [47]	6.6 ± 0.5	-

Table 1: The number of scans at a load on 0.44 N at a sliding speed of 4×10^{-3} m/s to decrease the C KLL Auger intensity to 1/e of its original value, S_e, for the adsorption of each of the carboxylic acids on copper, compared with the initial friction coefficient of the saturated overlayer of each compound.

Compound	Relative C/Cu Auger Ratio after Heating to 800 K	Relative C/Cu Auger Ratio after Rubbing
7-Octenoic Acid	0.47	0.12
Octanoic Acid	0.36	0.11

Table 2: The proportion of carbon remaining on the surface after a TPD experiment and after rubbing in ultrahigh vacuum.

Figure Captions

Figure 1: Analyses of the surface of the tungsten carbide tribopin. Figure A shows the initially contaminated pin showing predominantly carbon on the surface and the upper trace shows the effect of e-beam heating now revealing the presence of tungsten. Figure B shows an Al Kα X-ray photoelectron spectrum of the tungsten carbide pin that has been argon ion bombarded. Reproduced with permission from ref [54].

Figure 2: Plot of the C/Cu Auger ratio in the wear track of a saturated overlayer of 7-octenoic acid on a copper foil as a function of the number of passes at a normal load of 0.44 N and a sliding speed of 4×10^{-3} m/s, for 7-octanoic acid on a clean surface (■) and after a second dose of 7-octanoic acid on the previously rubbed surface (●).

Figure 3: Plot of the initial (indicated as 0 scan) and final (indicated as 50 scans) carbon to copper Auger ratio measured in the wear track after rubbing a copper surface saturated with 7-octenoic acid at a normal load of 0.44 N at a sliding speed of 4×10^{-3} m/s. Neither the copper surface nor the tungsten carbide pin were cleaned between scans so that each consecutive scan is for an interface that includes the accumulated carbon from previous scans.

Figure 4: Plot of the C/Cu Auger ratio in the wear track of a saturated overlayer of octanoic acid on a copper foil as a function of the number of passes at a normal load of 0.44 N and a sliding speed of 4×10^{-3} m/s, for octanoic acid on a clean surface (■) and after a second dose of octanoic acid on the previously rubbed surface (●).

Figure 5: Plot of the initial (indicated as 0 scan) and final (indicated as 50 scans) carbon to copper Auger ratio measured in the wear track after rubbing a copper surface saturated with octanoic acid at a normal load of 0.44 N at a sliding speed of 4×10^{-3} m/s. Neither the copper

surface nor the tungsten carbide pin were cleaned between scans so that each consecutive scan is for an interface that includes the accumulated carbon from previous scans.

Figure 6: Plot of the O/Cu Auger ratio in the wear track of a saturated overlayer of 7-octenoic acid (■) and octanoic acid (●) as a function of the number of passes at a normal load of 0.44 N and a sliding speed of 4×10^{-3} m/s. Included also are the results for 6-heptenoic acid (▲) and heptanoic acid (▼) on copper.

Figure 7: Plot of the evolution in the friction coefficient of a 7-octenoic acid overlayer on copper rubbed at a normal load of 0.44 N and a sliding speed of 4×10^{-3} m/s for an overlayer formed on a clean surface (■) and on a surface that has been dosed and rubbed six times (●).

Figure 8: Plot of the evolution in the friction coefficient of an octanoic acid overlayer on copper rubbed at a normal load of 0.44 N and a sliding speed of 4×10^{-3} m/s for an overlayer formed on a clean surface (■) and on a surface that has been dosed and rubbed six times (●).

Figure 9: Plot of the depth at the center of the wear track of saturated overlayers of octanoic (■) and 7-octenoic acid (●) on Cu(100) measured using a silicon AFM tip as a function of the number of passes at a normal load of 56 nN, corresponding to a normal stress at the center of the contact, σ_0, of 0.27 GPa, and a scanning velocity of 120 nm/s.

Figure 10: Distribution of pull-off forces for octanoic and 7-octenoic acid on Cu(100) measured using a silicon AFM tip.

Figure 11: Plot of the friction force of octanoic (black trace) and 7-octenoic acid (red trace) on Cu(100) measured using a silicon AFM tip as a function of the number of passes at a normal load of 56 nN, corresponding to a normal stress at the center of the contact, σ_0, of 0.27 GPa, and a scan velocity of 120 nm/s.

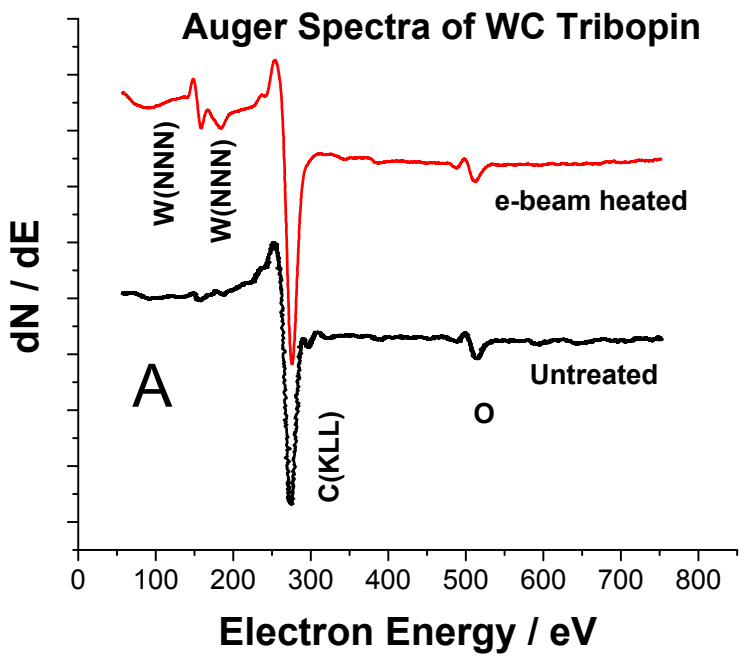

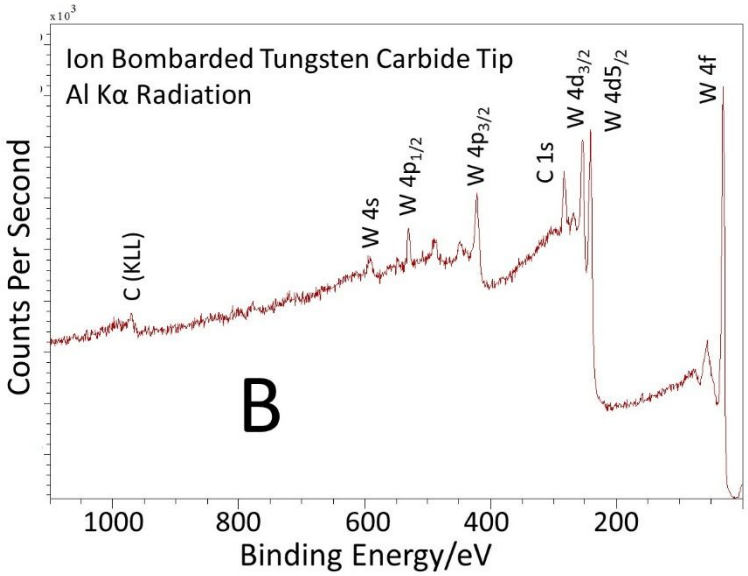

Rana et al, Figure 1

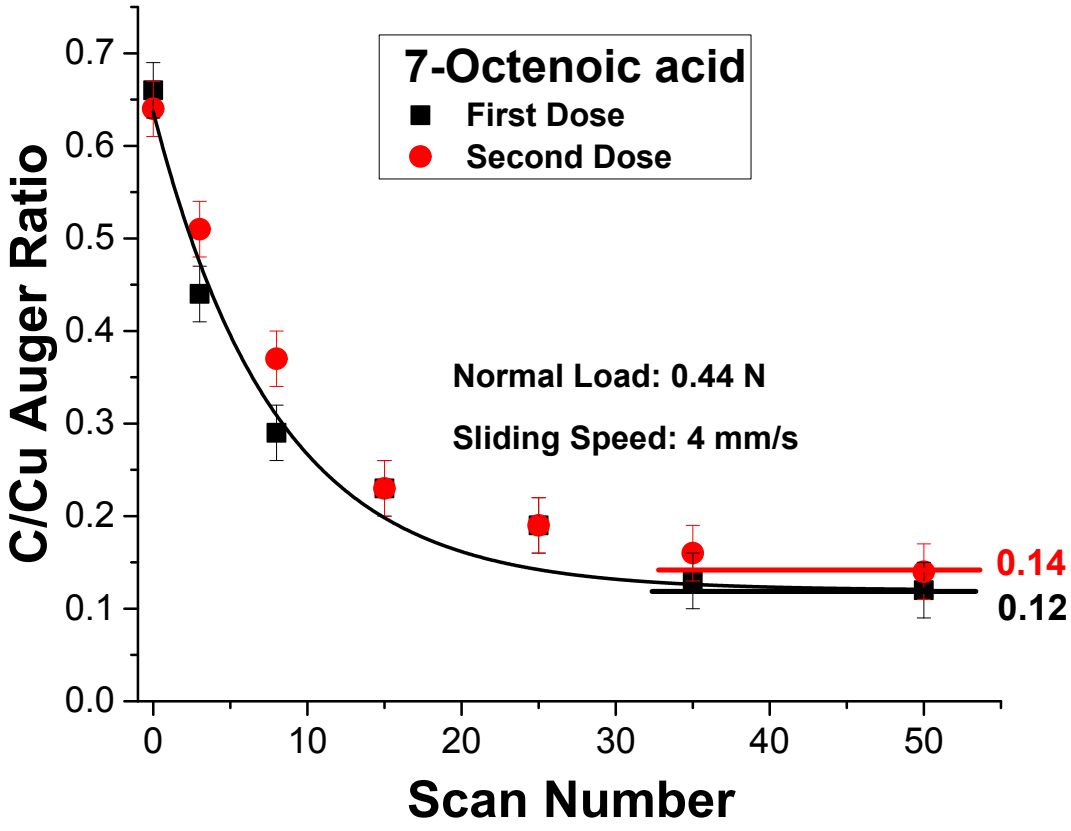

Rana et al, Figure 2

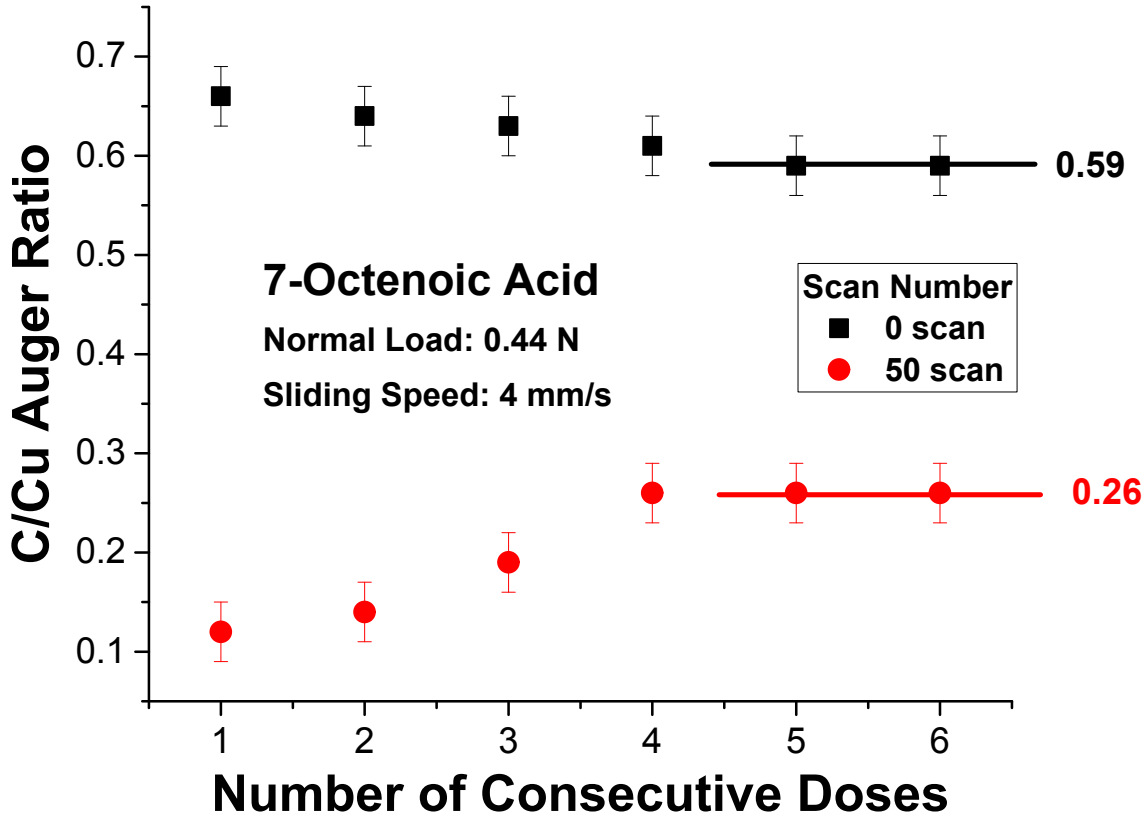

Rana et al, Figure 3

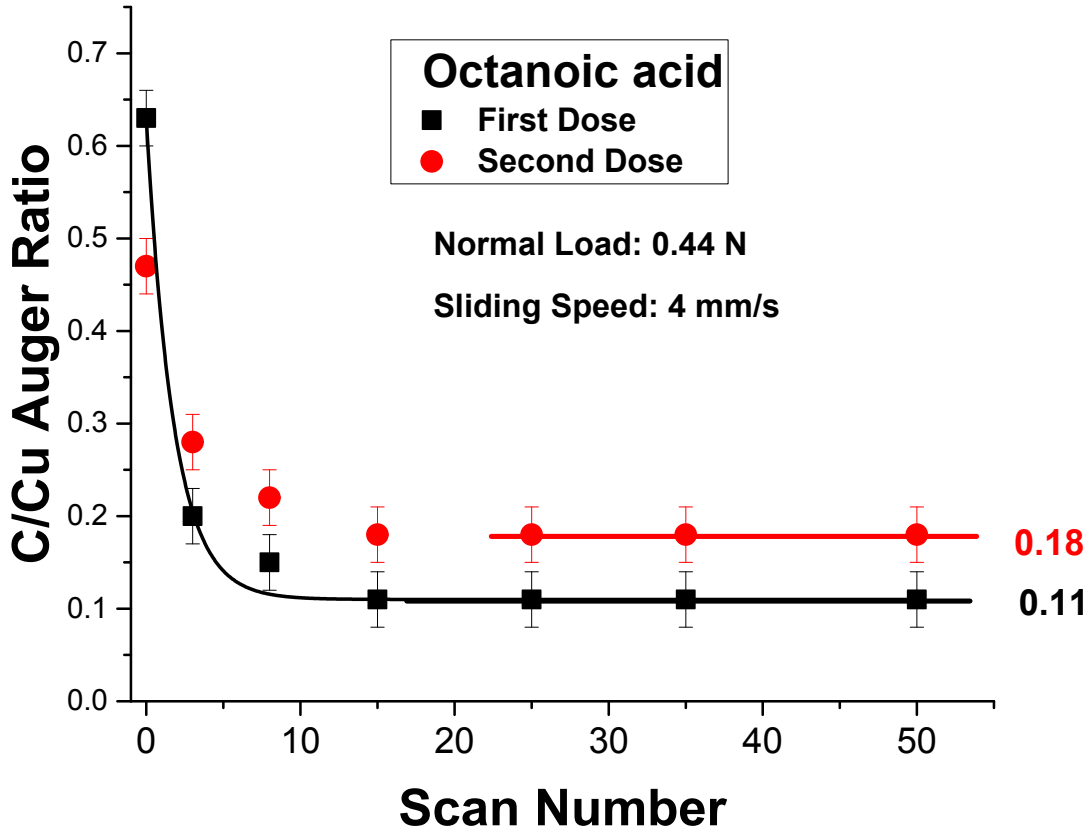

Rana et al, Figure 4

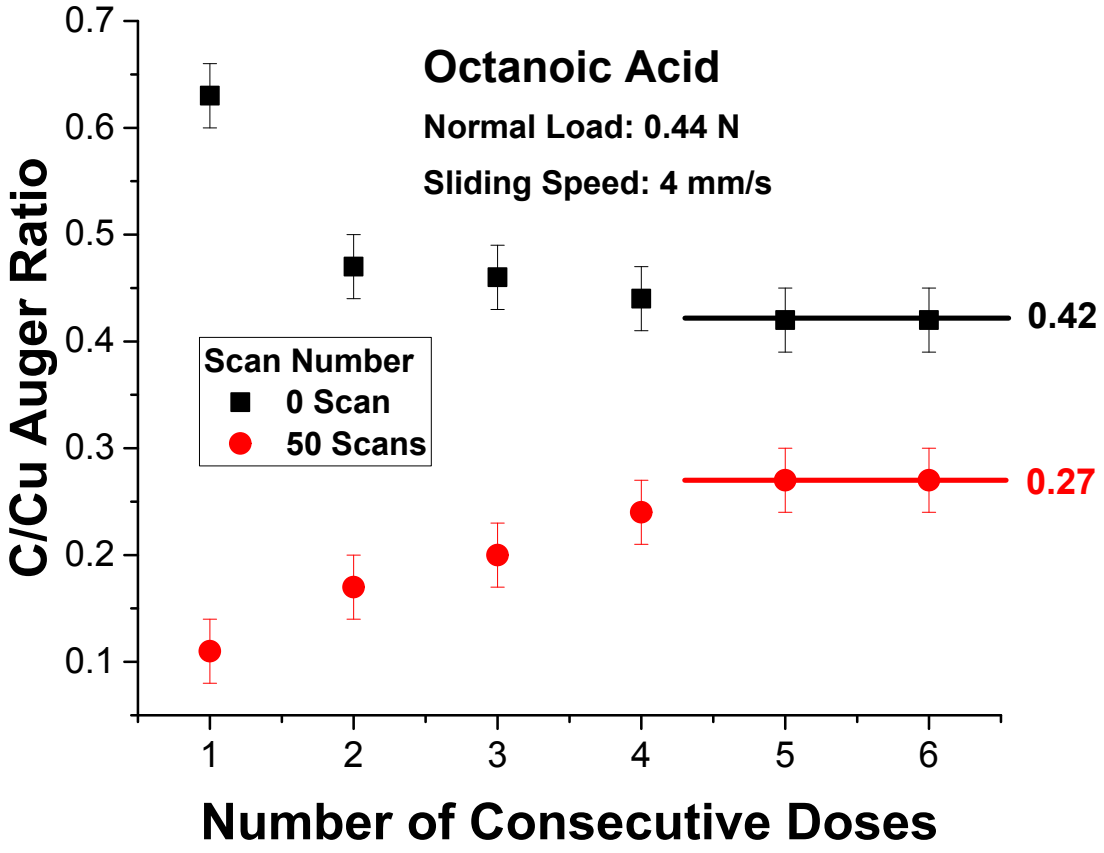

Rana et al, Figure 5

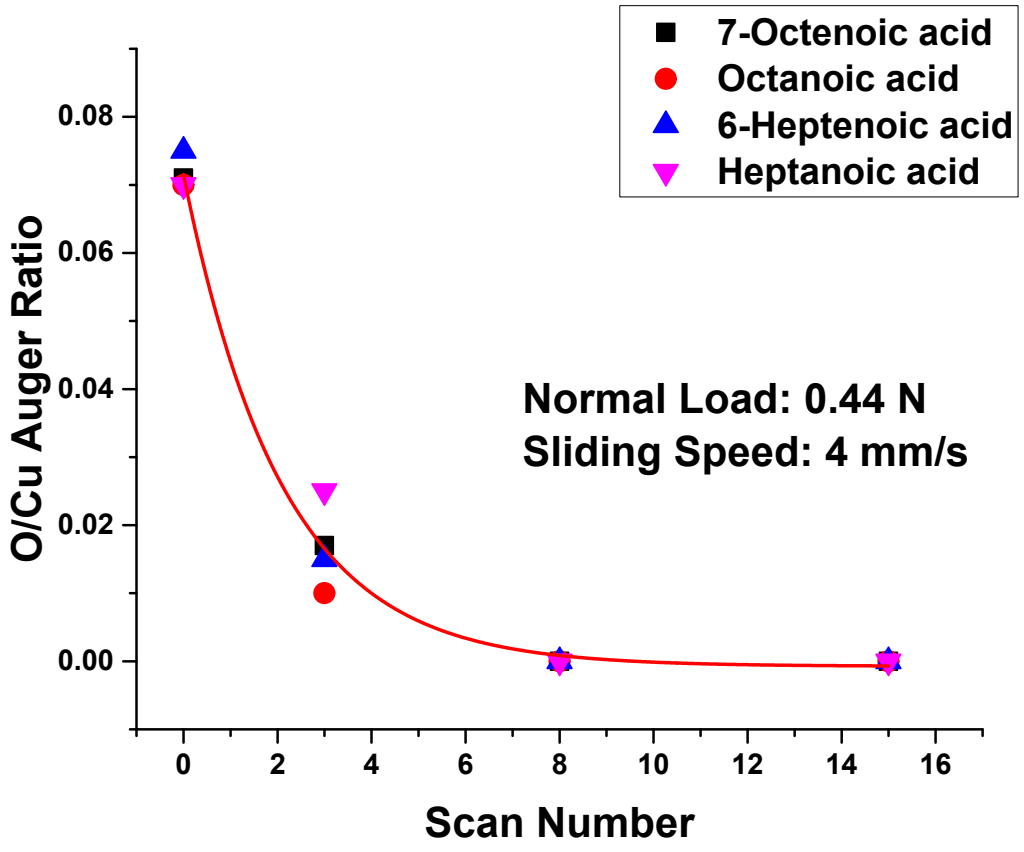

Rana et al, Figure 6

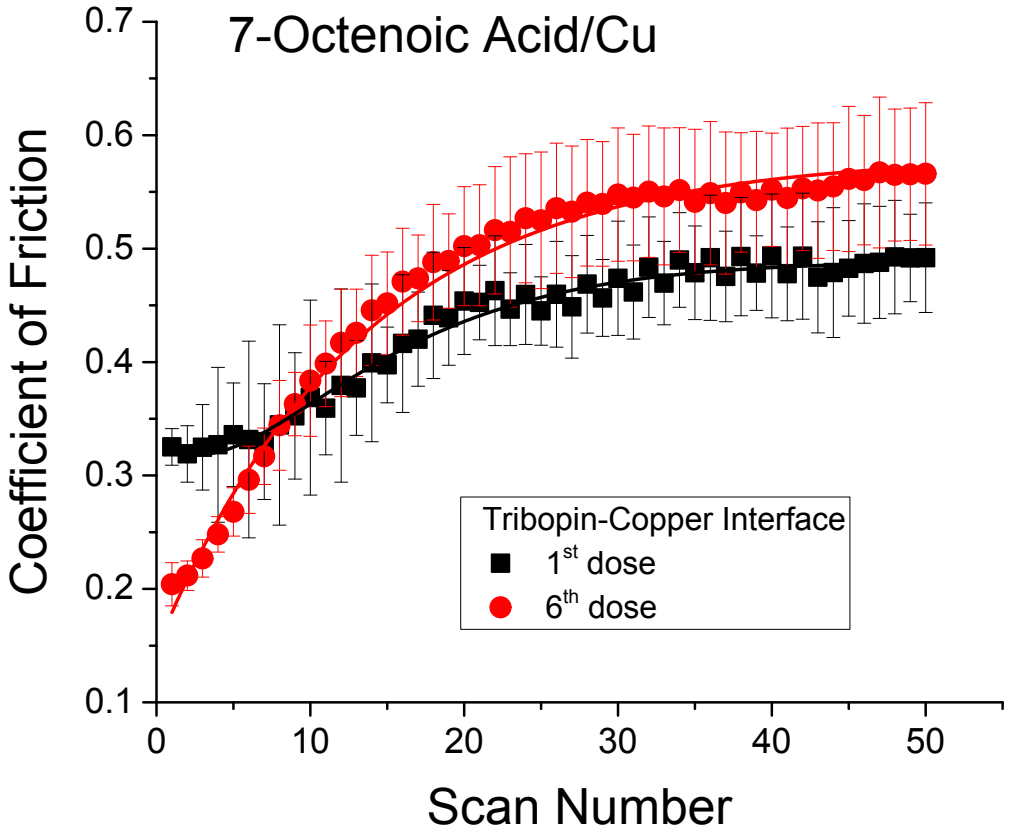

Rana et al, Figure 7

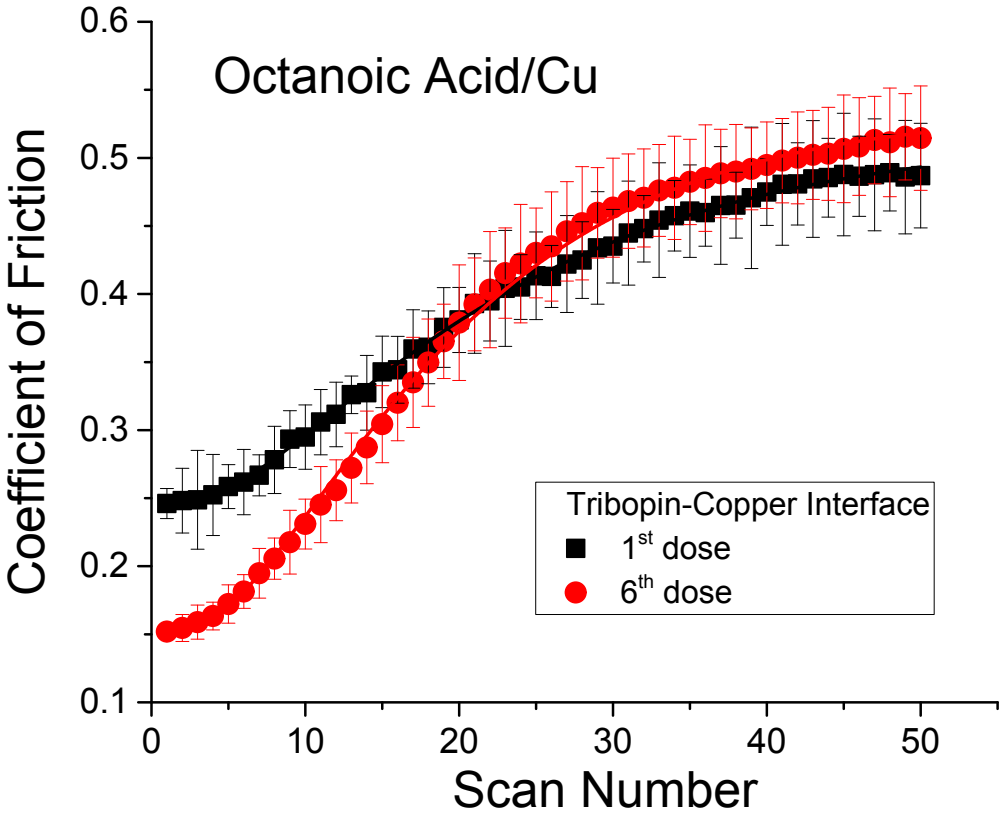

Rana et al, Figure 8

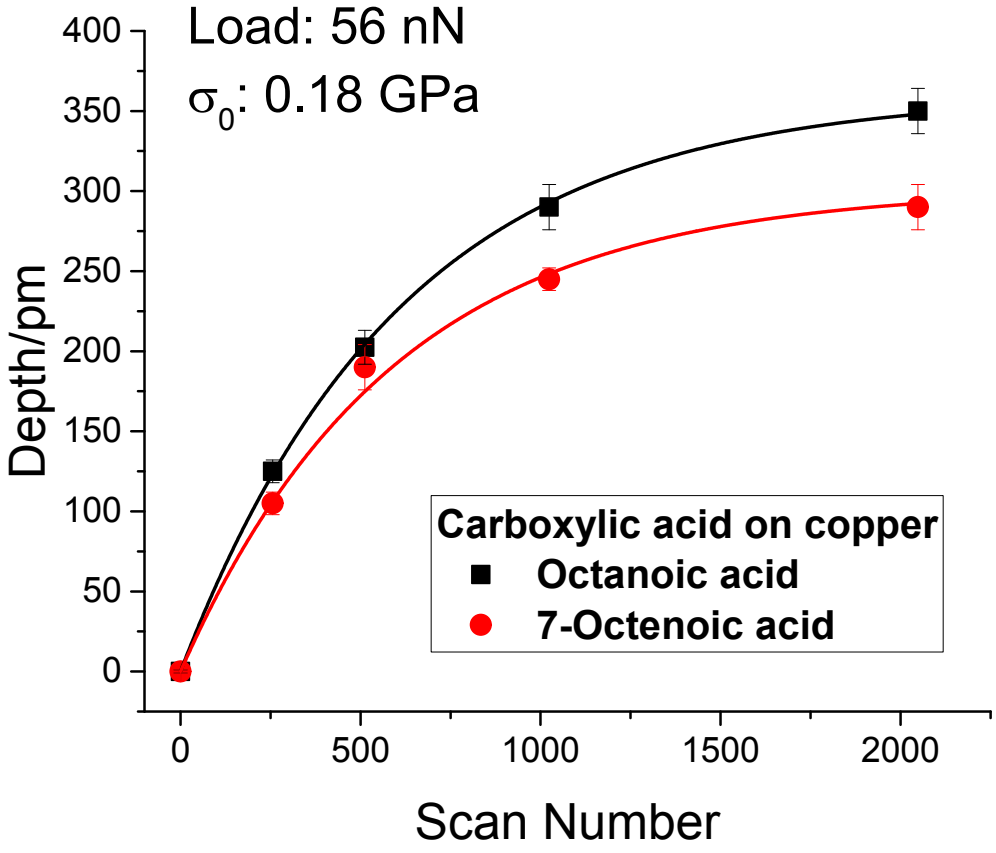

Rana et al, Figure 9

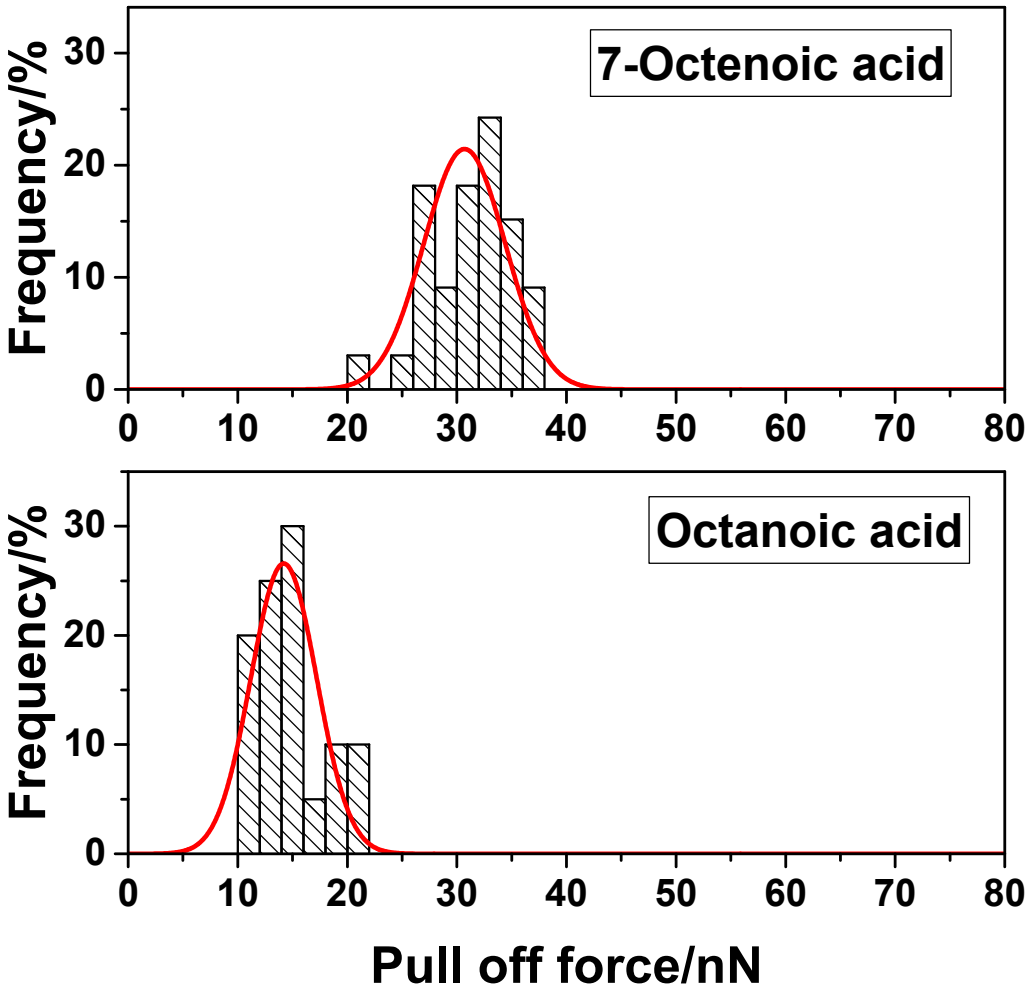

Rana et al, Figure 10

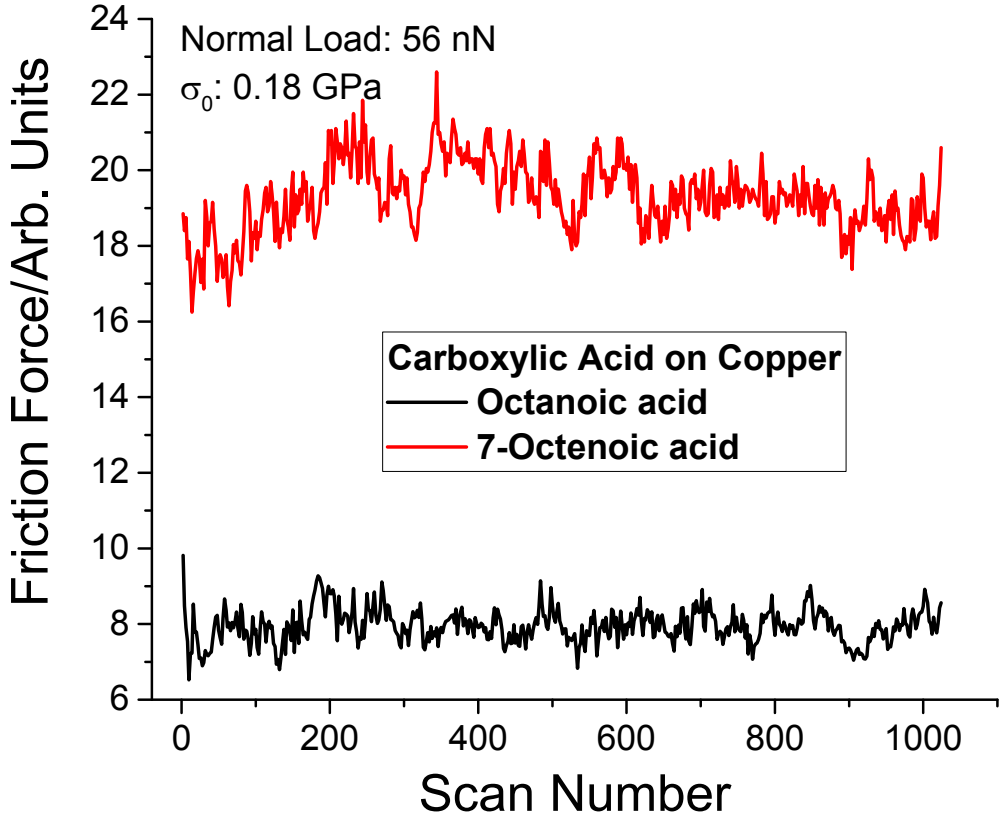

Rana et al, Figure 11